

**SMASIS2008-656**

## **CHARACTERIZATION AND MODELING OF DYNAMIC SENSING BEHAVIOR IN FERROMAGNETIC SHAPE MEMORY ALLOYS**

**Neelesh Sarawate**

Smart Vehicle Concepts Center  
Department of Mechanical Engineering  
The Ohio State University  
Columbus, Ohio 43210  
Email: sarawate.1@osu.edu

**Marcelo Dapino\***

Smart Vehicle Concepts Center  
Department Mechanical Engineering  
The Ohio State University  
Columbus, Ohio, 43210  
Email: dapino.1@osu.edu

### **ABSTRACT**

This paper is focused on the characterization and modeling of a commercial Ni-Mn-Ga alloy for use as a dynamic deformation sensor. The flux density is experimentally determined as a function of cyclic strain loading at frequencies from 0.2 Hz to 160 Hz. With increasing frequency, the stress-strain response remains almost unchanged whereas the flux density-strain response shows increasing hysteresis. This behavior indicates that twin-variant reorientation occurs in concert with the mechanical loading, whereas the rotation of magnetization vectors occurs with a delay as the loading frequency increases. The increasing hysteresis in magnetization must be considered when utilizing the material in dynamic sensing applications. A modeling strategy is developed which incorporates magnetic diffusion and a linear constitutive equation.

### **1 INTRODUCTION**

A major advantage of ferromagnetic shape memory alloys (FSMAs) in the Ni-Mn-Ga system over the thermally activated shape memory alloys (SMAs) is their ability to produce large strains of around 6% at high frequency bandwidth in the kHz range. Extensive work exists on the quasistatic behavior of these materials (see review papers [1,2]). However, the characterization and modeling of Ni-Mn-Ga under dynamic mechanical or magnetic excitation has received only limited attention.

Henry [3] presented measurements of magnetic field induced strains of up to 3% for drive field frequencies of up to 250 Hz and a linear model to describe the phase lag between strain and field and system resonance frequencies. Peterson [4] presented dynamic actuation measurements on piezoelectrically assisted twin boundary motion in Ni-Mn-Ga. The acoustic stress waves produced by a piezoelectric actuator complement the ex-

ternally applied fields and allow for reduced field strengths. Marioni et al. [5] presented pulsed magnetic field actuation of Ni-Mn-Ga for field pulses lasting up to 620  $\mu$ s. The complete field-induced strain was observed to occur in 250  $\mu$ s, indicating the possibility of obtaining cyclic 6% strain for frequencies of up to 2000 Hz. Magnetization measurements were not reported in these studies as they usually are not of great interest for actuation applications. Faidley et al. [6], and Sarawate and Dapino [7] presented frequency response measurements of acceleration transmissibility using mechanical base excitation to investigate the effect of bias fields on the stiffness of Ni-Mn-Ga. However, the magnitude of base acceleration was not sufficient to induce twin-boundary motion and associated magnetization changes.

The sensing effect in NiMnGa refers to the action of external mechanical stress on the magnetic properties of the material. Only a few studies exist on the sensing effect of Ni-Mn-Ga [8, 9, 10, 11, 12] as compared to the actuation effect. Mullner et al. [8] experimentally studied strain induced changes in the flux density under external quasistatic loading at a constant field of 558 kA/m. Straka and Heczko [9] reported superelastic response for fields higher than 239 kA/m and established the interconnection between magnetization and strain. Heczko [11] further investigated this interconnection and proposed a simple energy model. Suorsa et al. [10] reported magnetization measurements for various discrete strain and field intensities ranging between 0% and 6% and 5 and 120 kA/m, respectively. Sarawate and Dapino [12] reported flux density change due to 6% strain input at bias fields ranging from 0 to 445 kA/m, and presented a continuum thermodynamics model [13] for the sensing effect. However, all of these studies are concerned with quasistatic magnetization response, and an investigation on the effect of dynamic mechanical input on the magnetization of Ni-Mn-Ga has been lacking. Recently, Karaman et al. [14] reported voltage measurements in a pickup coil due to flux density change under dynamic strain loading of 4.9% at frequencies in the 0.5 to 10 Hz range,

---

\*Address all correspondence to this author.

from the viewpoint of energy harvesting. Their study presents the highest frequency of mechanical loading to date which induces twin boundary motion in Ni-Mn-Ga (10 Hz). However, the dependence of flux density on strain was not reported. We present the experimental characterization and modeling of the dynamic sensing behavior of Ni-Mn-Ga for frequencies of up to 160 Hz.

In this paper we characterize the dependence of flux density and stress on dynamic strain at a bias field of 368 kA/m for frequencies of up to 160 Hz, with a view to determining the feasibility of using Ni-Mn-Ga as a dynamic deformation sensor. This bias field was determined as optimum for obtaining maximum reversible flux density change [12]. The measurements also illustrate the dynamic behavior of twin boundary motion and magnetization rotation in Ni-Mn-Ga. A modeling strategy is developed using a linear constitutive equation and magnetic diffusion equation.

## 2 EXPERIMENTAL CHARACTERIZATION

Figure 1 shows the experimental setup, which consists of a custom designed electromagnet and a uniaxial MTS 831 test frame. This frame is designed for cyclic fatigue loading, with special servo valves which allow precise stroke control for frequencies of up to 200 Hz. The setup is similar to that described in Ref. [12] for characterization of the quasi-static sensing behavior. A  $6 \times 6 \times 10 \text{ mm}^3$  single crystal NiMnGa sample (AdaptaMat Ltd.) is placed in the center gap of the electromagnet. In the low-temperature martensite phase, the sample exhibits a free magnetic field induced deformation of 5.8% under a transverse field of 700 kA/m. The material is first converted to a single field-preferred variant by applying a high field along the transverse ( $x$ ) direction. The field is removed and the material is then slowly compressed 3.1% at a bias field of 368 kA/m applied in the  $x$  direction. While being exposed to the bias field, the sample is subjected to a cyclic uniaxial strain loading of 3% amplitude (peak to peak) along the longitudinal ( $y$ ) direction at a desired frequency. This process is repeated for frequencies ranging between 0.2 Hz and 160 Hz. The flux density inside the material is measured by a Hall probe placed in the gap between a magnet pole and a face of the sample. The Hall probe measures the net flux density along the  $x$ -direction, from which the  $x$ -axis magnetization can be calculated. The compressive force is measured by a load cell, and the displacement is measured by a linear variable differential transducer. The data is recorded using a dynamic data acquisition software at a sampling frequency of 4096 Hz. All the measuring instruments have a bandwidth in the kHz range, well above the highest frequency employed in the study.

Fig. 2(a) shows stress versus strain measurements for frequencies ranging from 4 Hz to 160 Hz. The strain axis is biased around the initial strain of 3.1%. These plots show typical pseudoelastic minor loop behavior associated with single crystal Ni-Mn-Ga at a high bias field. With increasing compressive strain, the stress increases elastically, until a critical value is reached, after which twin boundary motion starts and the stress-preferred variants grow at the expense of the field-preferred variants. During unloading, the material exhibits pseudoelastic reversible behavior because the bias field of 368 kA/m results in the genera-

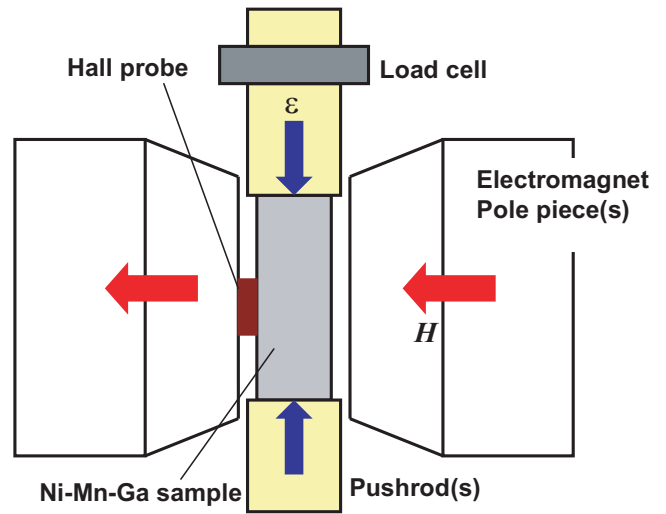


Figure 1. Experimental setup for dynamic magnetization measurements.

tion of field-preferred variants at the expense of stress-preferred variants.

The flux density dependence on strain shown in Fig. 2(b) is of interest for sensing applications. The absolute value of flux density decreases with increasing compression. During compression, due to the high magnetocrystalline anisotropy of Ni-Mn-Ga, the nucleation and growth of stress-preferred variants is associated with rotation of magnetization vectors into the longitudinal direction, which causes a reduction of the permeability and flux density in the transverse direction. At low frequencies of up to 4 Hz, the flux-density dependence on strain is almost linear with little hysteresis. This low-frequency behavior is consistent with some of the previous observations [11, 12, 15]. The net flux density change for a strain range of 3% is around 0.056 T (560 Gauss) for almost all frequencies, which shows that the magnetization vectors rotate in the longitudinal direction by the same amount for all the frequencies. The applied strain amplitude does not remain exactly at  $\pm 1.5\%$  because the MTS controller is working at very low displacements ( $\approx \pm 0.15 \text{ mm}$ ) and high frequencies. Nevertheless, the strain amplitudes are maintained within a sufficiently narrow range ( $\pm 8\%$ ) so that a comparative study is possible on a consistent basis for different frequencies.

With increasing frequency, the stress-strain behavior remains relatively unchanged (Fig. 2(a)). This indicates that the twin-variant reorientation occurs in concert with the applied loading for the frequency range under consideration. This behavior is consistent with work by Marioni [5] showing that twin boundary motion occurs in concert with the applied field for frequencies of up to 2000 Hz. On the other hand, the flux density dependence on strain shows a monotonic increase in hysteresis with increasing frequency. The hysteresis loss in the stress versus strain plots is equal to the area enclosed by one cycle ( $\oint \sigma d\epsilon$ ), whereas the loss in the flux density versus strain plots is obtained

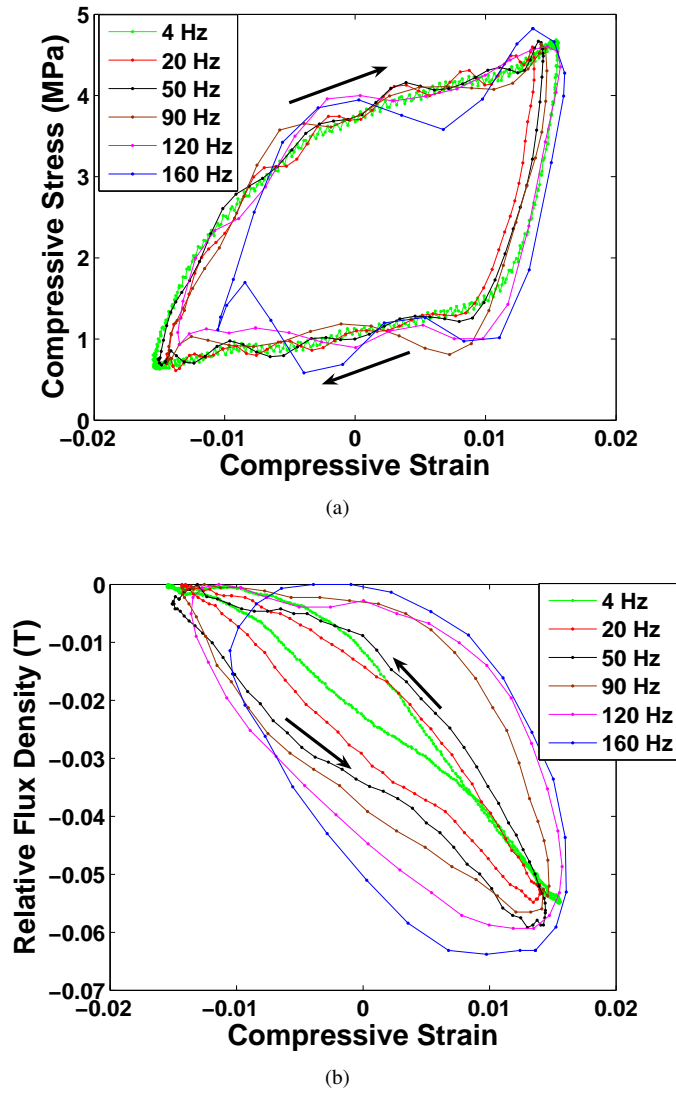


Figure 2. (a) Stress versus strain and (b) flux-density versus strain measurements for frequencies of up to 160 Hz.

by multiplying the enclosed area ( $\oint B d\epsilon$ ) by a constant that has units of magnetic field [16, 17]. Fig. 3 shows the hysteresis loss for the stress versus strain and the flux density versus strain plots. The hysteresis in the stress plots is relatively flat over the measured frequency range, whereas the hysteresis in the flux density increases about 10 times at 160 Hz compared to the quasistatic case. The volumetric energy loss, i.e., the area of the hysteresis loop is approximately linearly proportional to the frequency. The bias field of 368 kA/m is strong enough to ensure that the 180-degree domains disappear within each twin variant, hence each variant consists of a single magnetic domain throughout the cyclic loading process [13]. Therefore, the only parameter affecting the magnetization hysteresis is the rotation angle of the magnetization vectors with respect to the easy c-axis. This angle is independent of the strain and variant volume fraction [13], and is therefore a constant for the given bias field.

The process that leads to the observed magnetization depen-

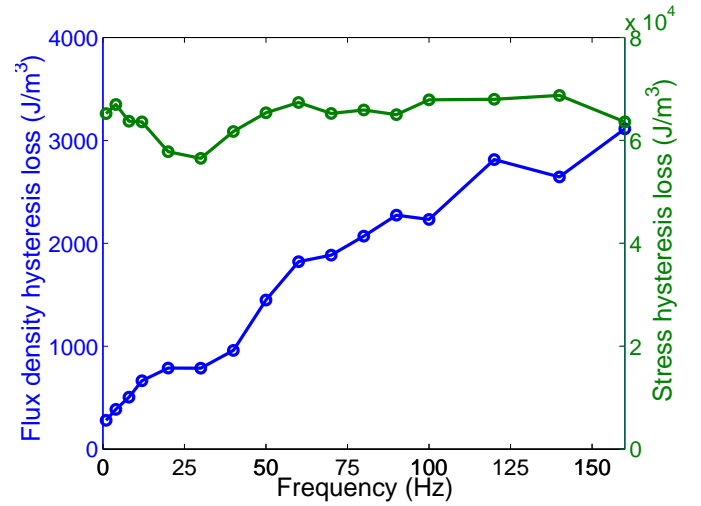


Figure 3. Hysteresis loss per volume versus frequency for stress versus strain and flux density versus strain.

dence on strain is postulated to occur in three steps: (i) As the sample is compressed, twin variant rearrangement occurs and the number of crystals with easy c-axis in the longitudinal (y) direction increases. The magnetization vectors remain attached to the c-axis, therefore the magnetization in these crystals is oriented along the y-direction. (ii) Subsequently, the magnetization vectors in these crystals rotate away from the c-axis to settle at a certain equilibrium angle defined by the competition between the Zeeman and magnetocrystalline anisotropy energies. This rotation process is proposed to occur according to the dynamics of a first order system. Time constants for first-order effects in Ni-Mn-Ga have been previously established for the time-dependent long-time strain response [18, 19], and strain response to pulsed field [5]. The time constant associated with pulse field response provides a measure of the dynamics of twin-boundary motion, which is estimated to be around  $157 \mu\text{s}$  [5]. In contrast, the time constant associated with magnetization rotation in our measurements is estimated to be around 1 ms. (iii) As the sample is unloaded, twin variant rearrangement occurs due to the applied bias field. Crystals with the c-axis oriented along the y-direction rotate into the x-direction, and an increase in the flux density along the x-direction is observed. At low frequencies, magnetization rotation occurs in concert with twin-variant reorientation. As the frequency increases, the delay associated with the rotation of magnetization vectors into their equilibrium position increases, which leads to the increase in hysteresis seen in Fig. 2(b). The counterclockwise direction of the magnetization hysteresis loops implies that the dynamics of magnetization rotation occur as described in steps (i)-(iii). If the magnetization vectors had directly settled at the equilibrium angle without going through step (i), the direction of the hysteresis excursions would have been clockwise.

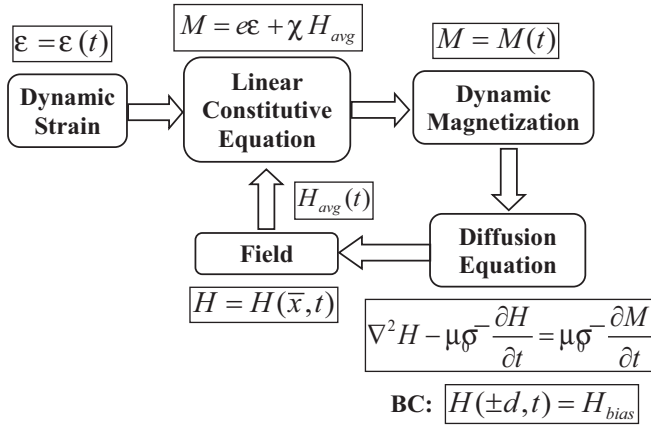


Figure 4. Strategy for modeling the frequency dependencies in magnetization-strain hysteresis.

### 3 MODEL FOR FREQUENCY DEPENDENT MAGNETIZATION VERSUS STRAIN HYSTERESIS

A continuum thermodynamics constitutive model has been developed to describe the quasi-static stress and flux density dependence on strain at varied bias fields [13]. The hysteretic stress versus strain curve is dictated by the evolution of the variant volume fractions. We propose that the evolution of volume fraction is independent of frequency for the given range, and therefore, no further modification is required to model the stress versus strain behavior at higher frequencies. However, the magnetization dependence on strain changes significantly with increasing frequencies due to the losses associated with the dynamic magnetization rotation resulting from mechanical loading. The modeling strategy is summarized in Figure 4.

The constitutive model [12] shows that at high bias fields, the dependence of flux density on strain is almost linear and non-hysteretic. Therefore, a linear constitutive equation for magnetization is assumed as an adequate approximation at quasi-static frequencies and modified to address dynamic effects. If the strain is applied at a sufficiently slow rate, the magnetization response can be approximated as follows,

$$M = e\varepsilon + \chi H_{avg} \quad (1)$$

where  $e$  and  $\chi$  are constants dependent on the given bias field. For the given data, these constants are estimated as,  $e = -4.58 \times 10^6$  A/m, and  $\chi = 2.32$ . The average field  $H_{avg}$  acting on the material is not necessarily equal to the bias field  $H_{bias}$ .

Equation (1) works well at low frequencies. However, as the frequency increases, consideration of dynamic effects becomes necessary. The dynamic losses are modeled using a 1-D diffusion equation that describes the interaction between the dynamic magnetization and the magnetic field inside the material,

$$\nabla^2 H - \mu_0 \bar{\sigma} \frac{\partial H}{\partial t} = \mu_0 \bar{\sigma} \frac{\partial M}{\partial t}, \quad (2)$$

This treatment is similar to that in Ref. [20] for dynamic

actuation, although the final form of the diffusion equation and the boundary conditions are different. The boundary condition on the two faces of the sample is the applied bias field,

$$H(\pm d, t) = H_{bias}. \quad (3)$$

Although the field on the edges of the sample is constant, the field inside the material varies as dictated by the diffusion equation. The diffusion equation is numerically solved using the backward difference method to obtain the magnetic field at a given position and time  $H(\bar{x}, t)$  inside the material.

For sinusoidal applied strain, the magnetization given by equation (1) varies in a sinusoidal fashion. This magnetization change dictates the variation of the magnetic field inside the material given by (2). The internal magnetic field thus varies in a sinusoidal fashion as seen in Figure 5(a). The magnitude of variation increases with increasing depth inside the material. In order to capture the bulk material behavior, the average of the internal field is calculated by,

$$H_{avg}(t) = \frac{1}{N_x} \sum_{\bar{x}=-\bar{x}_d}^{\bar{x}_d} H(\bar{x}, t), \quad (4)$$

where  $N_x$  represents the number of uniformly spaced points inside the material where the field waveforms are calculated.

Figure 5 shows the results of various stages in the model. The parameters used are,  $\mu_r=3.0$ , and  $\rho = 1/\bar{\sigma} = 62 \times 10^{-8}$  Ohm-m,  $N_x=40$ . Figure 5(a) shows the magnetic field at various depths inside the sample for a loading frequency of 140 Hz. It is seen that as the depth inside the sample increases, the variation of the magnetic field increases. At the edges of the sample ( $x = \pm d$ ), the magnetic field is constant, with a value equal to the applied bias field.

Figure 5(b) shows the variation of the average field at varied frequencies. The variation of the average field is directly proportional to the frequency of applied loading: as the frequency increases, the amplitude of the average field increases. Finally, the magnetization is recalculated by using the updated value of the average field as shown by the block diagram in Figure 4. The flux-density is obtained from the magnetization (see Figure 5(c)) by accounting for the demagnetization factor. It is seen that the model adequately captures the increasing hysteresis in flux density with increasing frequency. Further refinements in the model are possible, such as including a 2-D diffusion equation, and updating the permeability of the material while numerically solving the diffusion equation.

### 4 DISCUSSION

The magnetization and stress response of single-crystal Ni-Mn-Ga subjected to dynamic strain loading for frequencies from 0.2 Hz to 160 Hz is presented. This frequency range is significantly higher than previous characterizations of Ni-Mn-Ga

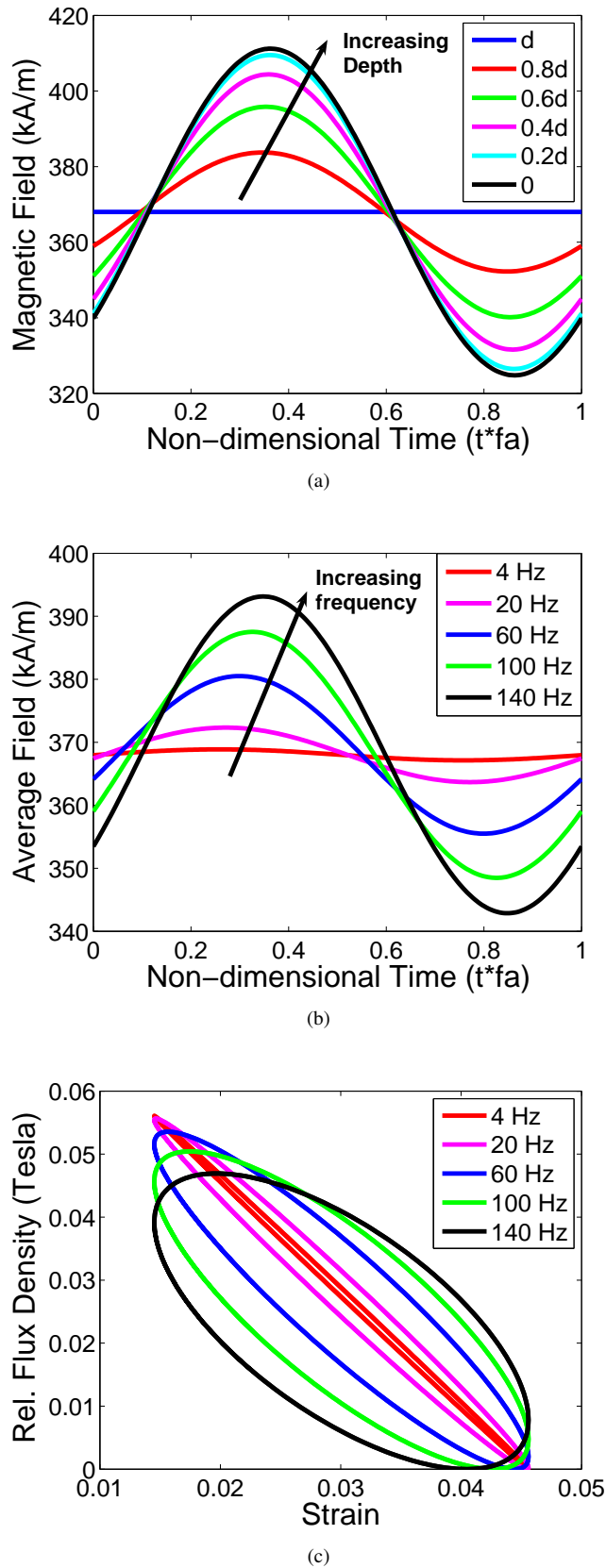


Figure 5. Model results: (a) Internal magnetic field versus time at varying depth for the case of 140 Hz strain loading (sample dim:  $\pm d$ ), (b) Average magnetic field versus time at varying frequencies, and (c) Flux-density versus strain at varying frequencies.

which investigated frequencies from d.c. to only 10 Hz. The rate of twin-variant reorientation remains unaffected by frequency; however, the rate of rotation of magnetization vectors away from the easy c-axis is lower than the rate of loading and of twin-variant reorientation. This behavior can be qualitatively explained by the dynamics of a first-order system associated with the rotation of magnetization vectors. The increasing hysteresis in the flux density could complicate the use of this material for dynamic sensing. However, the “sensitivity” of the material, i.e., net change in flux-density per percentage strain input remains relatively unchanged ( $\approx 190$  G per % strain) with increasing frequency. Thus the material retains the advantage of being a large-deformation, high-compliance sensor as compared to materials such as Terfenol-D [12] at relatively high frequencies. The significant magnetization change at structural frequencies also illustrates the feasibility of using Ni-Mn-Ga for energy harvesting applications. To employ the material as a dynamic sensor or in energy harvesting applications, permanent magnets can be used instead of an electromagnet. The electromagnet provides the flexibility of turning the field on and off at a desired magnitude, but the permanent magnets provide an energy efficiency advantage. The dynamic magnetization process in the material is modeled using a linear constitutive equation, along with a 1-D diffusion equation similar to that used a previous dynamic actuation model. The model adequately captures the frequency dependent magnetization versus strain hysteresis and describes the dynamic sensing behavior of Ni-Mn-Ga.

## ACKNOWLEDGEMENTS

This work was supported in part by the National Science Foundation under Grant CMS-0409512, Dr. Shih-Chi Liu, program director. We are grateful to the member organizations of the Smart Vehicle Concepts Center ([www.SmartVehicleCenter.org](http://www.SmartVehicleCenter.org)) and the National Science Foundation Industry/University Cooperative Research Centers program ([www.nsf.gov/eng/iip/iucr](http://www.nsf.gov/eng/iip/iucr)) for providing financial support. Additional support for N.S. was provided by the Smart Vehicle Concepts Center Fellowship Program.

## REFERENCES

- [1] Soderberg, O., Ge, Y., Sozniov, A., Hannula, S., and Lindroos, V. K., 2005. “Recent breakthrough development of the magnetic shape memory effect in NiMnGa alloys”. *Smart Materials and Structures*, **14**(5), pp. S223–S235.
- [2] Kiang, J., and Tong, L., 2005. “Modelling of magneto-mechanical behaviour of NiMnGa single crystals”. *Journal of Magnetism and Magnetic Materials*, **292**, pp. 394–412.
- [3] Henry, C., 2002. “Dynamic actuation response of Ni-Mn-Ga ferromagnetic shape memory alloys”. PhD thesis, Massachusetts Institute of Technology.
- [4] Peterson, B., 2006. “Acoustic assisted actuation of Ni-Mn-Ga ferromagnetic shape memory alloys”. PhD thesis, Massachusetts Institute of Technology.
- [5] Marioni, M., O’Handley, R., and Allen, S., 2003. “Pulsed



- magnetic field-induced actuation of NiMnGa single crystals". *Applied Physics Letters*, **83**(19), pp. 3966–3968.
- [6] Faidley, L. E., Dapino, M. J., Washington, G. N., and Lo-grasso, T. A., 2006. "Modulus Increase with Magnetic Field in Ferromagnetic Shape Memory NiMnGa". *Journal of Intelligent Material Systems and Structures*, **17**(2), pp. 123–131.
- [7] Sarawate, N., and Dapino, M., 2007. "Electrical stiffness tuning in ferromagnetic shape memory Ni-Mn-Ga". In *Proceedings of SPIE Smart Structures and Materials*, Vol. 6529, pp. 652916.1–11.
- [8] Mullner, P., Chernenko, V. A., and Kosterz, G., 2003. "Stress-induced twin rearrangement resulting in change of magnetization in a NiMnGa ferromagnetic martensite". *Scripta Materialia*, **49**(2), pp. 129–133.
- [9] Straka, L., and Heczko, O., 2003. "Superelastic Response of NiMnGa Martensite in Magnetic Fields and a Simple Model". *IEEE Transactions on Magnetics*, **39**(5), pp. 3402–3404.
- [10] Suorsa, I., Pagounis, E., and Ullakko, K., 2004. "Magnetization dependence on strain in the NiMnGa magnetic shape memory material". *Applied Physics Letters*, **84**(23), pp. 4658–4660.
- [11] Heczko, O., 2005. "Magnetic shape memory effect and magnetization reversal". *Journal of Magnetism and Magnetic Materials*, **290-291**(2), pp. 787–794.
- [12] Sarawate, N., and Dapino, M., 2006. "Experimental characterization of the sensor effect in ferromagnetic shape memory NiMnGa". *Applied Physics Letters*, **88**, pp. 121923.1–3.
- [13] Sarawate, N., and Dapino, M., 2007. "A continuum thermodynamics model for the sensing effect in ferromagnetic shape memory NiMnGa". *Journal of Applied Physics*, **101**(12), pp. 123522.1–11.
- [14] Karaman, I., Basaran, B., Karaca, H., Karsilayan, A., and Chumlyakov, Y., 2007. "Energy harvesting using martensite variant reorientation mechanism in a NiMnGa magnetic shape memory alloy". *Applied Physics Letters*, **90**, pp. 172505.1–3.
- [15] Li, G., Liu, Y., and Ngoi, B., 2005. "Some aspects of strain-induced change of magnetization in a NiMnGa single crystal". *Scripta Materialia*, **53**(7), pp. 829–834.
- [16] Uchino, K., and Hirose, S., 2001. "Loss Mechanisms in Piezoelectrics: How to Measure Different Losses Separately". *IEEE Transactions on Ultrasonics, Ferroelectrics, and Frequency Control*, **48**(1), pp. 307–321.
- [17] Ercuta, A., and Mihalca, I., 2002. "Magnetomechanical damping and magnetoelastic hysteresis in permalloy". *Journal of Physics D: Applied Physics*, **35**, pp. 2902–2908.
- [18] Glavatska, N., and L'vov, A. R. V., 2002. "Time-dependent magnetostrain effect and stress relaxation in the martensitic phase of NiMnGa". *Journal of Magnetism and Magnetic Materials*, **241**(2), pp. 287–291.
- [19] L'vov, V., Rudenko, O., and Glavatska, N., 2005. "Fluctuating stress as the origin of the time-dependent magnetostrain effect in Ni-Mn-Ga martensites". *Physical Review B*, **71**(2), pp. 024421.1–6.
- [20] Sarawate, N., and Dapino, M., 2008. "Frequency Dependent Strain-Field Hysteresis Model for Ferromagnetic Shape Memory NiMnGa". *IEEE Transactions on Magnetics*, **44**(5), pp. 566–575.